

Thermal Analyses for a Simplified Medium-Voltage Switchgear: Numerical and Experimental Benchmark Studies

Ahmet Efe Seker¹, Egemen Aslan Sakaci², Arif Deniz², Bayram Celik³ and Deniz Yildirim⁴

¹National Defense University, Hezarfen Aeronautics and Space Technologies Institute, Turkey
ahmetefeseker@outlook.com

²Siemens, Gebze Research and Development Center, Turkey
egemen.sakaci@siemens.com, arif.deniz@siemens.com

³Istanbul Technical University, Department of Astronautical Engineering, Turkey
celikbay@itu.edu.tr

⁴Istanbul Technical University, Department of Electrical Engineering, Turkey
yildiri1@itu.edu.tr

Abstract

Present study reports experimental and computational results obtained for a switchgear, where its critical components such as busbars, and tulip contacts are numerically modeled. In the experiment, thermocouples are used to measure the temperature at several locations of the switchgear at operating condition. One-way coupled EMAG and CFD computations are performed to obtain eddy current losses first, then the temperature and velocity distributions are obtained for the natural convection in and out of the model that is induced by the losses. Comparison of the obtained temperature distributions show that the experimental and computational results are in similar trend in general. In order to understand the causes of local discrepancies in the results, it is considered to conduct computations on a high performance computing environment for a more realistically modelled electrical components.

1. Introduction

Increasing demand for electrical energy has led to growth of energy grids. This growth causes increasing magnitude of short circuit currents and increases possible damage to electric devices [1]. Electrical devices which are operating with high currents can be safely connected or disconnected to grid with switchgears. In addition to that, switchgears also protect electrical devices from unexpected situations such as unstable conditions, overload and lightning [2].

Switchgears are generally classified as low, medium and high voltage by voltage class. Excluding this general classification, switchgears could be in various combinations depending on current rating, interrupting rating, insulating gas and more [3].

Due to its widespread use, there are number of numerical and experimental researches for different purposes about switchgears. In general, coupled or uncoupled, electromagnetic (EMAG) and computational fluid dynamics (CFD) analysis used in these researches. Ryfa et al. made a study about experimental determination of convective heat transfer coefficient. This study offers a new approach for the determination of the convective heat transfer coefficient. Expressions for new heat transfer coefficients that are based on reconciled data were proposed [4]. Bedkowski et al. used validated coupled CFD-EMAG model to simulate cooling enhancement of industrial low voltage switchgear. This study offers more complex busbar system instead of basic ones. The model results are compared with the measurements data for

two switchgear configurations. According to study, although grid layouts can be easily implemented, they have minor effects on reducing busbar temperature. Yet another output of this research is that radiation effects are significant on heat transfer [5]. Bedkowski et al. made another study about power loss generation of busbar system of low-voltage switchgear. In this study, uncoupled, one-way coupled, and two-way coupled solutions are considered, and their accuracy and numerical efficiency are compared. Even though two-way coupled model gives more realistic results than the others, it is significantly expensive in terms of computational time. The two-way coupled solution provided in [6], are in good agreement with the experimental data.

As mentioned here, different types of switchgears and solution approaches are considered in previous studies. These are not independent approaches but the steps of complete analysis. All of the steps offers a reliability within its limits. As steps gets complicated, precision, cost and computation time increase. The main objective of present study is to determine temperature distribution for a medium voltage (MV) switchgear. EMAG computations are first performed to determine electrical losses. Then thermal and flow fields are obtained by using CFD where the losses are used as an input to the computations in a one-way coupled fashion.

2. Experimental Setup

The objective of the test is to measure the temperature rises on the surfaces which are caused by the heat generation due to the power losses. Test object includes critical components of a switchgear such as busbars, tulip contacts and current transformers (CT). The test is made with 3 phases and 830 A rated operating current. Cross section of busbars is 600 mm² and three busbars are short circuited with a rectangular copper bar having equal cross sectional area. Thermocouples are connected to the surfaces of the critical components, connection parts and outer frame to measure the temperatures. Ambient temperature at the beginning of the test is also measured with a thermometer. Inner and outer sections of experimental setup model is shown in Fig. 1.

The test is finished when the temperature change is less than 1 Kelvin per hour. After the test is finished, the test object is kept for about 12 hours in the test laboratory before the next measurement in order to ensure that the temperature of all components become equivalent to the ambient temperature.

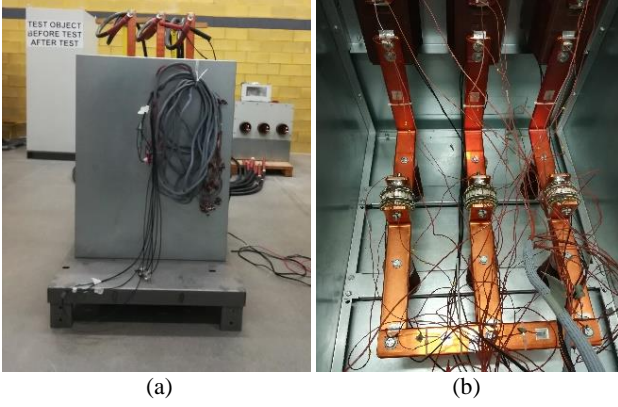


Fig. 1. Experimental setup model (a) outside view (b) inside view showing the thermocouple locations

The difference between the voltage drop values measured before test and after test shall not exceed 20%. Computational domain and thermocouple locations are shown in Fig. 2 [7].

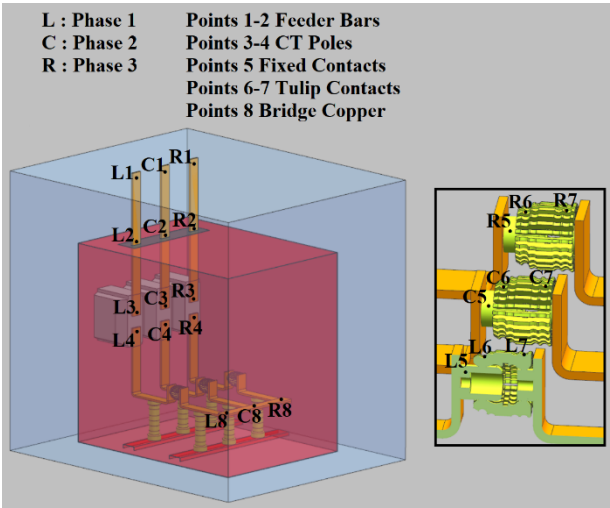


Fig. 2. Computational model and thermocouple locations

3. Computational Model

3.1. Finite Element Model

Computational model is generated by simplifying experimental model. There are some requirements for both EMAG and CFD analyses to reach an accurate solution. For instance, CFD modelling requires generation of specific meshes on the solid walls to resolve the high gradients in both thermal and velocity boundary layers. However, this requirement may bring some challenges in mesh generation due to the complex surfaces of the components as in this study.

In present study, computations for EMAG and CFD are one-way coupled and the prior one requires solution for whole computational domain. Therefore, the generated mesh must be appropriate for the computation. The solver used here requires two meshes to be identical. The computational mesh used in this study is shown in Fig. 3 where the boundary layers adjacent to the outer frame are meshed using hexahedral elements while the other regions are represented by tetrahedral elements.

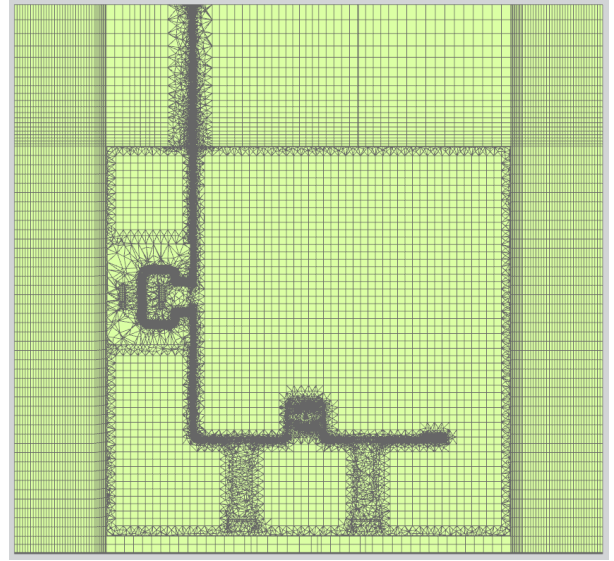


Fig. 3. Finite element model

3.2. EMAG Analysis

EMAG analysis require solution of Maxwell equations [8] below

$$\nabla \times \mathbf{H} = \mathbf{J} \quad (1)$$

$$\nabla \times \mathbf{E} = -\frac{\partial \mathbf{B}}{\partial t} \quad (2)$$

$$\mathbf{J} = \nabla \mathbf{E} \quad (3)$$

$$\nabla \cdot \mathbf{B} = 0 \quad (4)$$

where \mathbf{H} is the magnetic field strength, \mathbf{J} is the electric current density, \mathbf{E} is the electric field strength, \mathbf{B} is the magnetic flux density, and t is the time.

Commercial software of Siemens NX Magnetics solver can be used for the solutions of electrostatics, electrokinetics, electrodynamic, magnetostatics, magneto dynamic, and full wave problems. The benchmark problem that we model in this study requires solution of magnetodynamics numerically since the experimental model designed to run on three-phase alternating current. Magnetodynamics computations give magnetic field and eddy currents as outputs. Eddy currents contain losses due to the electrical resistivity and time-varying magnetic field [8]. The solver gives total losses for each element in the computational domain as a single output in W/mm^3 .

Material properties that are used in the EMAG analyses are tabulated in Table 1.

Top cover of outer frame is made of unsaturated polyester glass mat (UPGM). UPGM is not available on default material library, so it has created as a new material and its properties are introduced to the solver.

The only constraint used in the analyses is flux tangent that is used on the outer boundaries of the computational domain.

Table 1. Material Assignments

Material	Component
Electrolytic Copper	Busbar, CT Primary Conductor, Tulip Contact
Epoxy	Isolator, CT Block
Galvanized Steel	Outer Frame
UPGM	Insulated Top Cover

This constraint defines outer air volume boundaries and this definition sets zero vector potential on the boundaries. In EMAG computations the equations are solved in whole computational domain that includes solid and fluid regions [8]. This approach is essential because of nonignorable magnetic permeability of surrounding air.

Current and voltage source locations are given on busbar top faces. There are three busbars in computational model as shown in Fig. 2 where rated current values are defined on two of them and zero voltage is defined on the other one. Since busbars are connected to each other with a short circuit busbar, three phase currents can flow on all busbars.

After assigning materials properties and prescribing the boundary conditions given above, domain is ready to mesh. Mesh size has effects on accuracy and computational time. In general, decreasing mesh size increases accuracy and computational time. This fact is common for all analysis types. Besides that, in EMAG analysis most important point in meshing is using finer mesh on material transition areas since material properties change on these areas.

3.3. CFD Analysis

The losses that are obtained from the EMAG analysis are used as a heat source for the CFD analysis. Commercial software of Simcenter Thermal/Flow solver is used to carry out CFD analysis. The sources treated as boundary conditions on the solid surfaces that induce a buoyancy flow. The working fluid is air where continuities of mass, momentum, and energy equations are solved for the computational domain. The continuity, momentum, and energy equations in vector form are as follows:

$$\frac{\partial(\rho u)}{\partial x} + \frac{\partial(\rho v)}{\partial y} = 0. \quad (5)$$

$$\rho \left(u \frac{\partial u}{\partial x} + v \frac{\partial u}{\partial y} \right) = \mu \frac{\partial^2 u}{\partial y^2} - (\rho_{\infty} - \rho)g. \quad (6)$$

$$\rho C_p \left(u \frac{\partial T}{\partial x} + v \frac{\partial T}{\partial y} \right) = k \left(\frac{\partial^2 T}{\partial x^2} + \frac{\partial^2 T}{\partial y^2} \right). \quad (7)$$

where ρ is the density, u and v are the velocity vectors, μ is the dynamic viscosity, P is the pressure, C_p is the specific heat at constant pressure, T is the temperature, and k is the thermal conductivity [9].

In order to determine whether the flow is laminar or not for a natural convection, Rayleigh number is calculated. Rayleigh number is product of Prandtl number and Grashof numbers. Prandtl number is defined as the ratio of momentum diffusivity to thermal diffusivity. Grashof number is ratio of buoyant forces to viscous forces which used to determine air flow condition in natural convection. The expressions of Grashof and Rayleigh numbers are given below.

$$Gr_L = \frac{g\beta(T_s - T_{\infty})L^3}{\nu^2}. \quad (8)$$

$$Ra_L = Gr_L Pr. \quad (9)$$

where g is the gravitational acceleration, β is the coefficient of volume expansion, T_s is temperature on the solid surface, T_{∞} is temperature of the fluid sufficiently far from the surface, L is characteristic length, ν is the kinematic viscosity, and Pr is Prandtl number. If Rayleigh number greater than 10^9 , air flow is considered to be turbulent. Grashof number can also be used for determination of boundary layer thickness according to the Eq. 10 [9].

$$\delta = \frac{6L}{\sqrt[4]{Gr_L}} \quad (10)$$

where δ is boundary layer thickness. The parameters used in the calculations are based on the experiment and they are listed in the Table 2.

Table 2. Parameters Adapted from the Experiment

Symbol	Parameter	Value
g	Gravitational Acceleration	9.81 m/s ²
T _s	Surface Temperature	75.0 °C
T _∞	Air Temperature	25.8 °C
β	Thermal Expansion Coefficient of Air	3.09E-03 K ⁻¹
L	Characteristic Length	750 mm
ν	Kinematic Viscosity of Air	1.82E-05 m ² /s
Gr	Grashoff Number	1.89E+09
Pr	Prandtl Number	0.704
Ra	Rayleigh Number	1.33E+09
δ	Boundary Layer Thickness	30.52 mm

The characteristic length, L that appears in the table is height of the outer frame. According to the calculated Ra , the flow becomes turbulent at the end of the frame approximately. Therefore, the flow is assumed to be laminar in present study. In order to resolve laminar boundary layer, especially for the growing boundary layers adjacent to the outer surfaces of the frame, the computational mesh that consists of hexahedral elements with a growing factor of 1.05 is generated. To reduce computational costs, tetrahedral elements are used in the region where the flow velocities are relatively low.

On the solid surfaces no-slip and adiabatic boundary condition are prescribed. At the outer surfaces of the computational domain zero gradient boundary condition is applied for flow and thermal solvers [10]. Convection to environment constraint is defined at the top surfaces of the busbars. This constraint aims to modelling cables that are connected to the top of the busbars.

One-way coupled nature of the problem requires to use identical mesh for the CFD and EMAG. In CFD root mean square (RMS) residuals are tracked to check convergency. The steady state solutions discussed below are obtained with the residuals that are lower than 10^{-5} .

4. Results

In order to obtain eddy currents, EMAG analysis is performed. As residuals are approximately on the order of 10^{-9} , computational model is considered to be converged. Eddy current loss density is shown in Fig. 4 where losses are intensified on edges of busbars. Total losses of system including busbars, CT primary conductors, tulip contacts and outer frame are equal to 200 W.

The Eddy current losses that were obtained from the EMAG computations were used as sources in CFD computations. After solving continuity, momentum, and energy equations numerically, velocity and temperature distributions in the computational domain were obtained.

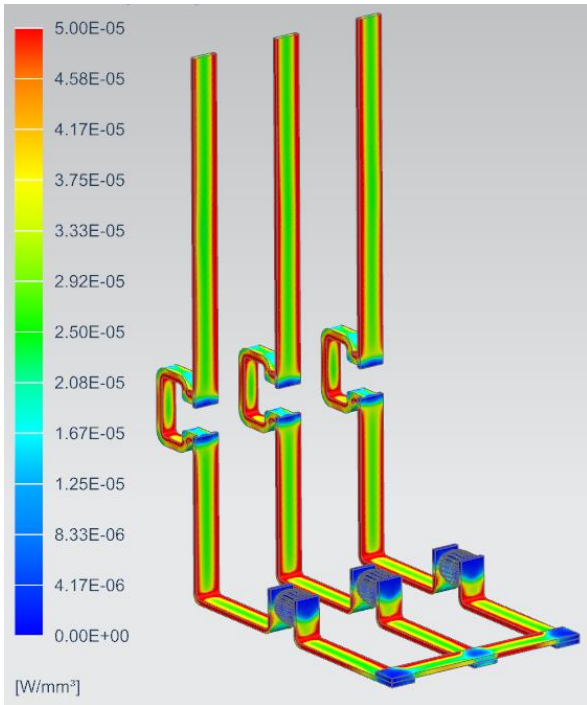


Fig. 4. Eddy current loss density at rated current

The streamlines colored with the velocity magnitudes and final temperature distributions on the solid surfaces excluding the frame are shown in Figs. 5 and 6, respectively. The computations were continued until the maximum deviation in the temperature dropped below 0.25 °C. As can be seen from the Fig. 5, developing thermal and velocity boundary layers form on the external sides of the frame due to the buoyancy flow. On the other hand, the internal flow field is 3-dimensional, where there is a large recirculation region appears on the upper right of the frame.

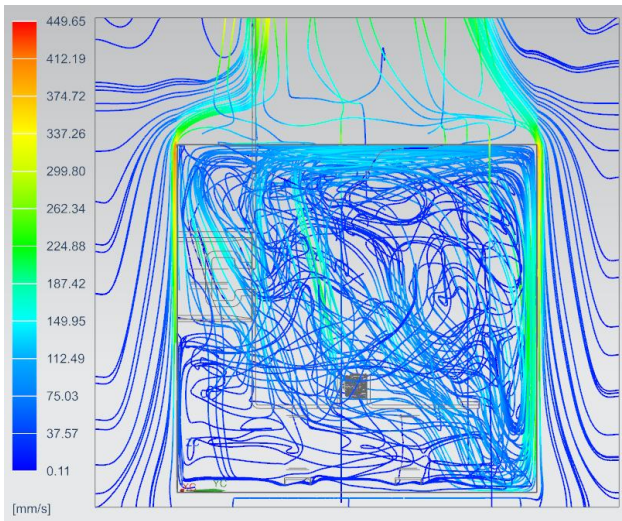


Fig. 5. Air flow velocities

In order to compare the computational results with the experimental one quantitatively, the temperature values are given in Fig. 7 for the specific location that are shown in Fig. 2.

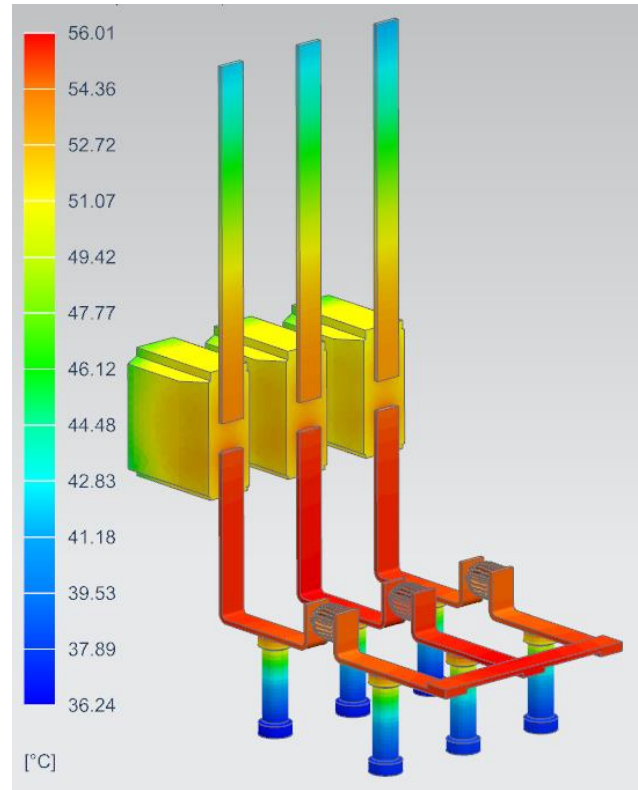


Fig. 6. Steady state temperature distribution

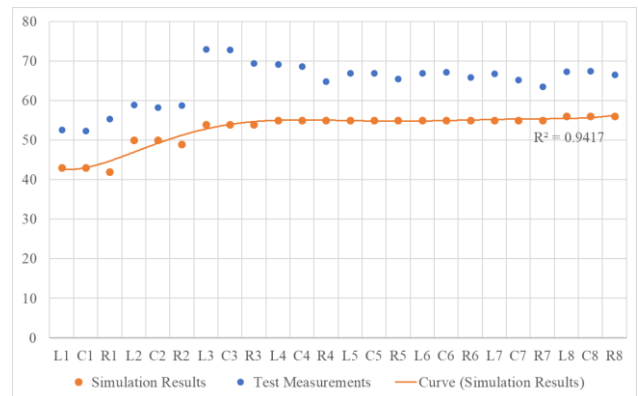


Fig. 7. Comparison of measurement and numerical results

In general, the results show similar trends but there are significant differences near the current transformer. This observation requires further computation and analysis, where more realistic modelling approach for the transformer might be applied.

5. Conclusions

In conclusion, this study is focused on observing the temperature distribution on specified points of the conductors, the air flow behavior inside the enclosure and the verification of simulation results with experiment. Electromagnetic losses, obtained in EMAG, are taken as thermal load input to CFD, which are very important for accuracy of the results. Although the study is performed on a simplified model, it gives several hints for complicated designs of MV switchgear. Without doing several

experiments, we can improve the design knowing the air flow behavior and the hottest spots along the current path.

Main reasons for the difference between simulation and experimental results are simplifications on 3D model (especially on conductors), mesh quality, electromagnetic/thermal properties of materials which are dependent on temperature and not being able to implement all experimental conditions to simulation environment. Our further study will focus on more complicated designs and on improving accuracy of the results. Accuracy of the results are considered to be improved by giving extra boundary conditions on electrical components (current transformer, tulip contacts, etc.) or modelling them with more details and observing experiments carefully in order to apply all constraints as boundary conditions for both EMAG and CFD. In addition, two-way coupled simulation will be performed to take into account the temperature dependencies of material properties. Meshing will be still key factor and will be optimized in terms of accuracy and computing time.

Acknowledgment

This study is initiated and funded by Siemens and academically supported by İTÜNOVA Technology Transfer Office with contract number EM-02-N-01-19-12-N-QQM-227259-13272. The authors thank to test engineers Mr. Utku Barış Kalkancı and Hilmi Coşkun Öztürk of Siemens A.Ş. for support on obtaining experimental results and Siemens Gebze R&D group manager Tahsin Karadeniz for his valuable contributions and assistance.

6. References

- [1] L. Song, "Transformer Short Circuit Current Calculation and Solutions", B.S. thesis, Elec. Eng., Novia Univ. App. Sci., Vaasa, SE, 2013.
- [2] Siemens AG. (2019, Sep 3). *Power Engineering Guide* (8.0) [Document]. Available: <https://profiles.siemens.com/pub/downloads/get?formSubmitGuid=6cf24691-de3e-45f7-aaaa-91eb6a250a76>.
- [3] R. W. Smeaton, "Switchgear and Control Handbook", 3rd Ed., McGraw Hill, New York, USA, 1997.
- [4] A. Ryfa, J. Smolka, Z. Bulinski, M. Bedkowski, "Experimental determination of the convective heat transfer coefficient for a switchgear busbar system with a use of the data reconciliation method", *Applied Thermal Engineering*, vol. 136, pp. 541-547, Mar, 2018.
- [5] M. Bedkowski, J. Smolka, Z. Bulinski, A. Ryfa, "Simulation of cooling enhancement in industrial low-voltage switchgear using validated coupled CFD-EMAG model", *International Journal of Thermal Sciences*, vol. 111, pp. 437-449, Sep, 2016.
- [6] M. Bedkowski, J. Smolka, K. Banasiak, Z. Bulinski, A. J. Nowak, T. Tomanek, A. Wajda, "Coupled numerical modelling of power loss generation in busbar system of low-voltage switchgear", *International Journal of Thermal Sciences*, vol. 82, pp. 122-129, May, 2014.
- [7] *High-voltage switchgear and controlgear – Part 1: Common specifications for alternating current switchgear and controlgear*, IEC 62271-1, July 2017.
- [8] R. Anderl, P. Binde, "Simulations with NX", Carl Hanser Verlag, Munich, Germany, 2014.
- [9] F. P. Incropera, D. P. DeWitt, "Fundamentals of heat and mass transfer", J. Wiley, New York, USA, 2002.
- [10] Siemens Documentation. (2019, Sep 3). *Flow Boundary Condition Types* [Document]. Available: https://docs.plm.automation.siemens.com/tdoc/nx/12.0.2/nx_help/#uid:xid1128419:index_advanced:xid389653:xid1282594:id1126372:id631661:id631681